

Local Linear Forests

Rina Friedberg
rsf@stanford.edu

Julie Tibshirani
julietibs@gmail.com

Susan Athey
athey@stanford.edu

Stefan Wager
swager@stanford.edu

Draft Version July 31, 2018

Abstract

Random forests are a powerful method for non-parametric regression, but are limited in their ability to fit smooth signals, and can show poor predictive performance in the presence of strong, smooth effects. Taking the perspective of random forests as an adaptive kernel method, we pair the forest kernel with a local linear regression adjustment to better capture smoothness. The resulting procedure, *local linear forests*, enables us to improve on asymptotic rates of convergence for random forests with smooth signals, and provides substantial gains in accuracy on both real and simulated data.

1 Introduction

Random forests [Breiman, 2001] are a popular method for non-parametric regression that have proven effective across many application areas [Cutler et al., 2007, Díaz-Uriarte and De Andres, 2006, Svetnik et al., 2003]. A major weakness of random forests, however, is their inability to exploit smoothness in the regression surface they are estimating. As an example, consider the following setup with a smooth trend in the mean: We simulate X_1, \dots, X_n independently from the uniform distribution on $[0, 1]^{20}$, with responses

$$Y_i = \log(1 + e^{6X_{i1}}) + \varepsilon_i, \quad \varepsilon_i \sim \mathcal{N}(0, 20), \quad (1)$$

and our goal is to estimate $\mu(x) = \mathbb{E}[Y | X = x]$. The left panel of Figure 1 shows a set of predictions on this data from a random forest. The forest is unable to exploit strong local trends and, as a result, fits the target function using qualitatively the wrong shape: the prediction surface resembles a step function as opposed to a smooth curve.

In order to address this weakness, we take the perspective of random forests as an adaptive kernel method. This interpretation follows work by Athey et al. [2018], Hothorn et al. [2004], and Meinshausen [2006], and complements the traditional view of forests as an ensemble method (i.e., an average of predictions made by individual trees). Specifically, random forest predictions can be written as

$$\hat{\mu}_{\text{rf}}(x) = \sum_{i=1}^n \alpha_i(x) Y_i, \quad \sum_{i=1}^n \alpha_i(x) = 1, \quad \alpha_i(x) \geq 0, \quad (2)$$

where the weights $\alpha_i(x)$ defined in (6) encode the weight given by the forest to the i -th training example when predicting at x . Now, as is well-known in the literature on non-parametric regression, if we want to fit smooth signals without some form of neighborhood averaging (e.g., kernel regression, k -NN, or matching for causal inference), it is helpful to use a local regression adjustment to correct for potential misalignment between a test point and its neighborhood [Abadie and Imbens, 2011, Cleveland and Devlin, 1988, Fan and Gijbels, 1996, Heckman et al.,

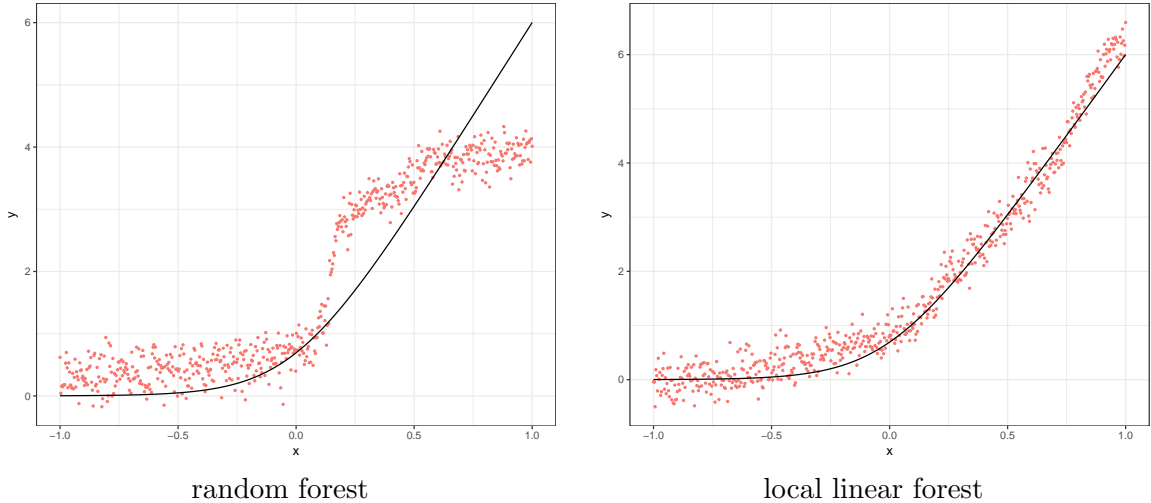


Figure 1: Predictions from random forests and local linear forests on 600 test points. Training and test data were simulated from equation (1), with dimension $d = 20$ and errors $\varepsilon \sim N(0, 20)$. Forests were trained on $n = 600$ training points using the R package `grf` [Tibshirani et al., 2018] and tuned via cross-validation. Here the true conditional mean signal $\mu(x)$ is in black, and predictions are shown in red.

1998, Loader, 1999, Newey, 1994, Stone, 1977, Tibshirani and Hastie, 1987]. These types of adjustments are particularly important near boundaries, where neighborhoods are asymmetric by necessity, but with many covariates, the adjustments are also important away from boundaries given that local neighborhoods are often unbalanced due to sampling variation. The goal of this paper is improve the accuracy of forests on smooth signals using regression adjustments, potentially in many dimensions. By using the local regression adjustment, it is possible to adjust for asymmetries and imbalances in the set of nearby points used for prediction, ensuring that the weighted average of the feature vector of neighboring points is approximately equal to the target feature vector, and that predictions are centered. The use of regression adjustments further implies that the remaining prediction error is due to strong local curvature in the data generating process. The improvement to forests from the regression adjustment is most likely to be large in cases where some features have strong effects with moderate curvature, so that regression adjustments are both effective and important. Many datasets from economics have this characteristic; for example, labor market outcomes tend to improve with parents' educational and labor market attainment, but there are diminishing returns.

In their simplest form, local linear forests just take the forest weights $\alpha_i(x)$, and use them for local regression:

$$\begin{pmatrix} \hat{\mu}(x) \\ \hat{\theta}(x) \end{pmatrix} = \operatorname{argmin}_{\mu, \theta} \left\{ \sum_{i=1}^n \alpha_i(x) (Y_i - \mu(x) - (X_i - x)\theta(x))^2 + \lambda \|\theta(x)\|_2^2 \right\}. \quad (3)$$

Here $\hat{\mu}(x)$ estimates the conditional mean function $\mu(x)$, and $\theta(x)$ corrects for the local trend in $X_i - x$. The ridge penalty $\lambda \|\theta(x)\|_2^2$ prevents overfitting to the local trend, and plays a key role both in simulation experiments and asymptotic convergence results. Then, as discussed in Section 2.1, we can improve the performance of local linear forests by modifying the tree-splitting procedure used to get the weights $\alpha_i(x)$, and making it account for the fact that we will use local regression to estimate $\mu(x)$. As a first encouraging result we note that, in the motivating example from Figure 1, local linear forests have essentially eliminated the bias of standard forests.

We can also consider our approach from the starting point of local linear regression. Despite working well in low dimensions, classical approaches to local linear regression are not applicable

to even moderately high-dimensional problems.¹ In contrast, random forests are adept at fitting high-dimensional signals, both in terms of their stability and computational efficiency. From this perspective, random forests can be seen as an effective way of producing weights to use in local linear regression.

Local linear forests aim to combine the strength of random forests in fitting high dimensional signals, and the ability of local linear regression to capture smoothness. We explore the properties of this procedure from both a theoretical and an empirical perspective, and find that it presents a promising alternative to traditional random forests.

1.1 Motivating Example: Attitudes to Welfare

For conciseness, this paper focuses on local linear forests for non-parametric regression; however, as discussed in Section 2.4, a similar local linear correction can also be applied to quantile regression forests [Meinshausen, 2006], causal forests [Wager and Athey, 2018] or, more broadly, to any instance of generalized random forests [Athey, Tibshirani, and Wager, 2018]. To highlight this potential, we start our discussion with an example of heterogeneous treatment effect estimation using local linear causal forests.

As in Wager and Athey [2018], we frame our discussion in terms of the Neyman-Rubin causal model [Imbens and Rubin, 2015]. Suppose we have data (X_i, Y_i, W_i) , where X_i are covariates, $Y_i \in \mathbb{R}$ is the response, and $W_i \in \{0, 1\}$ is the treatment. In order to define the causal effect of the treatment W_i , we posit potential outcomes for individual i , $Y_i(0)$ and $Y_i(1)$, corresponding to the response the subject would have experienced in the control and treated conditions respectively; we then observe $Y_i = Y_i(W_i)$. We seek to estimate the conditional average treatment effect (CATE) of W , namely $\tau(x) = \mathbb{E}[Y(1) - Y(0) \mid X = x]$. Assuming unconfoundedness [Rosenbaum and Rubin, 1983],

$$\{Y_i(0), Y_i(1)\} \perp\!\!\!\perp W_i \mid X_i, \quad (4)$$

the CATE is in general identified via non-parametric methods. We assume unconfoundedness when discussing treatment effect estimation through this paper. Wager and Athey [2018] proposed an extension of random forests for estimating CATEs, and Athey et al. [2018] improved on the method by making it locally robust to confounding using the transformation of Robinson [1988]. Here, we propose a local linear correction to the method of Athey et al. [2018] to strengthen its performance when $\tau(\cdot)$ is smooth; see Section 2.4 for details.

To illustrate the value of the local linear causal forests, we consider a popular dataset from the General Social Survey (GSS) that explores how word choice reveals public opinions about welfare. Individuals filling out the survey from 1986 to 2010 answered whether they believe the government spends too much, too little, or the right amount on the social safety net.² GSS randomly assigned the wording of this question, such that the social safety net was either described as “welfare” or “assistance to the poor”. This change had a well-documented effect on responses due to the negative perception many Americans have about welfare; moreover, there is evidence of heterogeneity in the CATE surface [Green and Kern, 2012].

Here, we write $W_i = 1$ if the i -th sample received the “welfare” treatment, and define $Y_i = 1$ if the i -th response was that the government spends too much on the social safety net. Thus, a positive treatment effect $\tau(x)$ indicates that, conditionally on $X_i = x$, using the phrase “welfare” as opposed to “assistance to the poor” increases the likelihood that the i -th subject says the government spends too much on the social safety net. We base our analysis on $d = 12$ covariates, including income, political views, age, and number of children. The full dataset has $N = 28,646$ observations; here, to make the problem interesting, we test our method on smaller subsamples of the data.

¹The curse of dimensionality for kernel weighting is well known. The popular core R function `loess` [R Core Team, 2018] allows only 1-4 predictors, while `locfit` [Loader, 2013] crashes on the simulation from (1) with $d \geq 7$.

²See <https://gssdataexplorer.norc.umd.edu/variables/191/vshow>

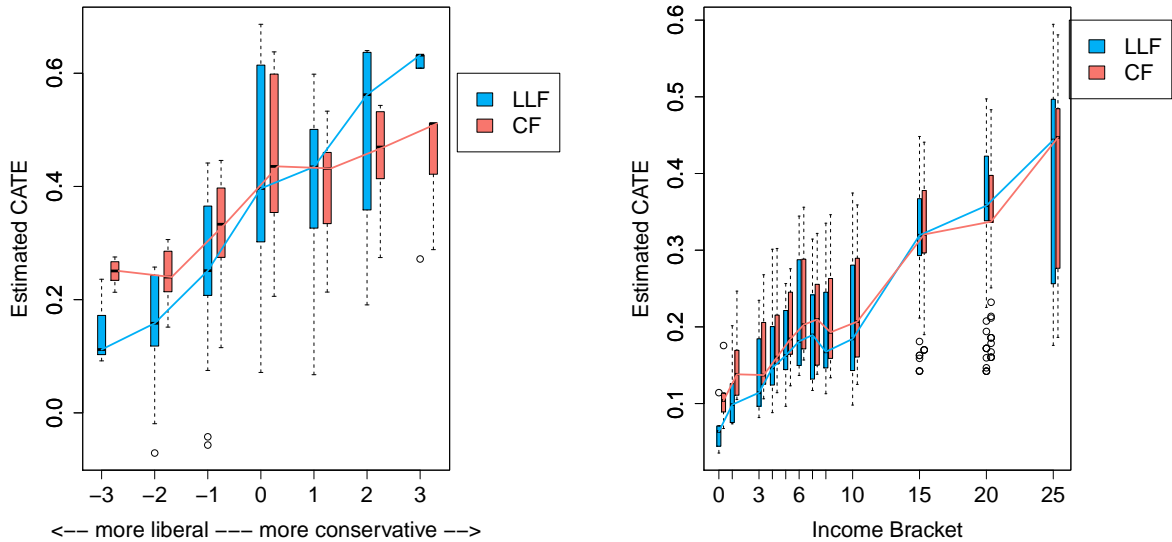


Figure 2: Estimated trends in CATE of welfare language by political views (left) and by income (right). On the x -axis is the bracket of either political views or income, and the boxplots show test set predictions $\hat{\tau}(X_i)$ from local linear causal forests and causal forests. Solid lines connect the medians of each boxplot. Each forest was trained on 400 subsampled training points, with cross-validation, and evaluated on 1000 test points.

Figure 2 displays the CATE by categories of income and political views, as estimated by both a local linear causal forest and a plain causal forest using $n = 600$ observations, again both implemented using `grf`. The display suggests that local linear causal forests are able to exploit smoothness and monotonicity to reveal more heterogeneity along these important features, which may mean that the local linear correction is helping.

In order to compare the performance of both methods more formally, we use the transformed outcome metric of [Athey and Imbens \[2015\]](#). Noting that $\mathbb{E}[(2W_i - 1)Y_i] = \tau(X_i)$, they suggest examining the following test set error criterion

$$\mathcal{E} = \frac{1}{|\mathcal{S}_{test}|} \sum_{i \in \mathcal{S}_{test}} ((2W_i - 1)Y_i - \hat{\tau}(X_i))^2, \quad (5)$$

$$\mathbb{E}[\mathcal{E}] = \mathbb{E}[(\tau(X) - \hat{\tau}(X))^2] + S_0, \quad S_0 = \mathbb{E}[(2W_i - 1)Y_i - \tau(X_i)]^2.$$

If we can estimate S_0 , then (5) gives an unbiased estimate of the mean-squared error of $\hat{\tau}(\cdot)$. Here, we estimate S_0 via out-of-bag estimation on the full dataset with $N = 28,646$, assuming that a local linear forest with such a large sample size has negligible error.

Table 1 has error estimates for both types of forests using (5), and verifies that using the local linear correction improves empirical performance across different subsample sizes. Section 4 contains a more detailed simulation study of local linear causal forests, comparing them with a wider array of baseline methods.

1.2 Related Work

Random forests were first introduced by [Breiman \[2001\]](#), building on the work of [Breiman, Friedman, Stone, and Olshen \[1984\]](#) on recursive partitioning (CART), [Breiman \[1996\]](#) on bagging, and [Amit and Geman \[1997\]](#) on randomized trees. [Bühlmann and Yu \[2002\]](#) shows how the bagging makes forests smoother than single trees, while [Biau \[2012\]](#) and [Scornet, Biau, and](#)

Subsample size	200	400	800	1200	1500	2000
CF	0.035	0.021	0.015	0.014	0.011	0.007
LLCF	0.027	0.017	0.013	0.013	0.011	0.006

Table 1: Estimated MSE of estimating the treatment effect on subsampled welfare data, averaged over 200 runs at each subsample size. Here we have calculated the estimated in sample MSE (5). We show estimated test error from local linear causal forests (LLCF) and standard causal forests (CF). Tuning parameters were selected via cross-validation estimating $\hat{\tau}$ by regressions on the control and treatment variables separately.

Vert [2015] establishes asymptotic risk consistency of random forests under specific assumptions. Mentch and Hooker [2016] and Wager, Hastie, and Efron [2014] propose methods for uncertainty quantification in random forests, while Wager and Athey [2018] prove a central limit theorem for forests that allows for asymptotically valid confidence intervals. More sophisticated tree-based ensembles motivated by random forests have been proposed by Zhou and Hooker [2018], who consider a hybrid between random forests and boosting, and Zhu, Zeng, and Kosorok [2015], who do deeper search during splitting to mitigate the greediness of CART.

The idea of considering random forests as an adaptive kernel method has been proposed by several papers. Hothorn et al. [2004] suggest using weights from survival trees and gives compelling simulation results, albeit to our knowledge no theoretical guarantees. Meinshausen [2006] proposes this technique for quantile regression forests and gives asymptotic consistency of the resulting predictions. Athey, Tibshirani, and Wager [2018] leverage this idea to present generalized random forests as a method for solving heterogeneous estimating equations. They derive an asymptotic distribution and confidence intervals for the resulting predictions. Local linear forests build on this literature; the difference being being that we use the kernel-based perspective on forests to exploit smoothness of $\mu(\cdot)$ rather than to target more complicated estimands (such as a quantile).

Our work is motivated by the literature local linear regression and maximum likelihood estimation [Abadie and Imbens, 2011, Cleveland and Devlin, 1988, Fan and Gijbels, 1996, Heckman et al., 1998, Loader, 1999, Newey, 1994, Stone, 1977, Tibshirani and Hastie, 1987]. Stone [1977] introduces local linear regression and gives asymptotic consistency properties. Cleveland [1979] expands on this by introducing robust locally weighted regression, and Fan and Gijbels [1992] give a variable bandwidth version. Cleveland and Devlin [1988] explore further uses of locally weighted regression. Local linear regression has been particularly well-studied for longitudinal data, as in Li and Hsing [2010] and Yao, Muller, and Wang [2005]. Cheng, Fan, and Marron [1997] use local polynomials to estimate the value of a function at the boundary of its domain. Abadie and Imbens [2011] show how incorporating a local linear correction improves nearest neighbor matching procedures.

2 Local Linear Forests

Local linear forests use a random forest to generate weights that can then serve as a kernel for local linear regression. Suppose we have training data $(X_1, Y_1), \dots, (X_n, Y_n)$ with $Y_i = \mu(X_i) + \varepsilon_i$, for $\varepsilon_i \sim N(0, \sigma^2)$. Consider using a random forest to estimate the conditional mean function $\mu(x) = \mathbb{E}[Y \mid X = x]$ at test point x . Traditionally, random forests are viewed as an ensemble method, where tree predictions are averaged to obtain the final estimate. Specifically, for each tree T_b in a forest of B trees, we find the leaf $L_b(x)$ with predicted response $\hat{\mu}_b(x)$, which is simply the average response of all training data points assigned to $L_b(x)$. We then predict the average $\hat{\mu}(x) = \frac{1}{B} \sum_{b=1}^B \hat{\mu}_b(x)$.

An alternate angle, advocated by Athey et al. [2018], Hothorn et al. [2004], and Meinshausen [2006], entails viewing random forests as adaptive weight generators, as follows. Equivalently

write $\hat{\mu}_b(x)$ as

$$\begin{aligned}\hat{\mu}(x) &= \frac{1}{B} \sum_{b=1}^B \sum_{i=1}^n Y_i \frac{1\{X_i \in L_b(x)\}}{|L_b(x)|} \\ &= \sum_{i=1}^n Y_i \frac{1}{B} \sum_{b=1}^B \frac{1\{X_i \in L_b(x)\}}{|L_b(x)|} = \sum_{i=1}^n \alpha_i(x) Y_i,\end{aligned}$$

where the forest weight $\alpha_i(x)$ is

$$\alpha_i(x) = \frac{1}{B} \sum_{b=1}^B \frac{1\{X_i \in L_b(x)\}}{|L_b(x)|} \quad (6)$$

Notice that by construction, $\sum_{i=1}^n \alpha_i(x) = 1$ and for each i , $0 \leq \alpha_i(x) \leq 1$. [Athey et al. \[2018\]](#) use this perspective to harness random forests for solving weighted estimating equations, and give asymptotic guarantees on the resulting predictions.

Local linear forests solve the locally weighted least squares problem (3) with weights (6). Note that equation (3) has a closed-form solution, as follows. Throughout this paper, we let A be the diagonal matrix with $A_{i,i} = \alpha_i(x)$, and let J denote the $d+1 \times d+1$ diagonal matrix with $J_{1,1} = 0$ and $J_{i+1,i+1} = A_{i,i}$, so as to not penalize the intercept. We define Δ , the centered regression matrix with intercept, as $\Delta_{i,1} = 1$ and $\Delta_{i,j+1} = X_{i,j} - x_j$. Then the local linear forest estimator can be explicitly written as

$$\begin{pmatrix} \hat{\mu}(x) \\ \hat{\theta}(x) \end{pmatrix} = (\Delta^T A \Delta + \lambda J)^{-1} \Delta^T A Y \quad (7)$$

Qualitatively, we can think of local linear regression as a weighting estimator with a modulated weighting function $\gamma_i \alpha_i(x)$ whose X -moments are better aligned with the test point x : $\hat{\mu}(x) = \sum_{i=1}^n \gamma_i \alpha_i(x) Y_i$ with $\sum_{i=1}^n \gamma_i \alpha_i(x) = 1$ and $\sum_{i=1}^n \gamma_i \alpha_i(x) X_i \approx x$, where the last relation would be exact without a ridge penalty (i.e., with $\lambda = 0$).

With the perspective of generating a kernel for local linear regression in mind, we move to discuss the appropriate splitting rule for local linear forests.

2.1 Splitting for Local Regression

Random forests traditionally use Classification and Regression Trees (CART) from [Breiman et al. \[1984\]](#) splits, which proceed as follows. We consider a parent node P with n_P observations $(X_{i1}, Y_{i1}), \dots, (X_{in_P}, Y_{in_P})$. For each candidate pair of child nodes C_1, C_2 , we take the mean value of Y inside each child, \bar{Y}_1 and \bar{Y}_2 . Then we choose C_1, C_2 to minimize the sum of squared errors

$$\sum_{i: X_i \in C_1} (Y_i - \bar{Y}_1)^2 + \sum_{i: X_i \in C_2} (Y_i - \bar{Y}_2)^2$$

Knowing that we will use the forest weights to perform a local regression, we neither need nor want to use the forest to model strong, smooth signals; the final regression step can model the strong global effects. Instead, in the parent node P , we run a ridge regression to predict Y_{ik} from X_{ik} .

$$\hat{Y}_{ik} = X_{ik}^T \hat{\beta}_P, \quad \text{for } \hat{\beta}_P = (X_P^T X_P + \lambda J)^{-1} X_P^T Y_P \quad (8)$$

We then run a standard CART split on the residuals $Y_{ik} - \hat{Y}_{ik}$, modeling local effects in the forest and regressing global effects back in at prediction.

To explore the effects of CART and residual splitting rules, we consider this simulation first introduced by [Friedman \[1991\]](#). Generate X_1, \dots, X_n independently and identically distributed $U[0, 1]^5$ and model Y_i from

$$y = 10 \sin(\pi x_1 x_2) + 20(x_3 - 0.5)^2 + 10x_4 + 5x_5 + \epsilon, \quad (9)$$

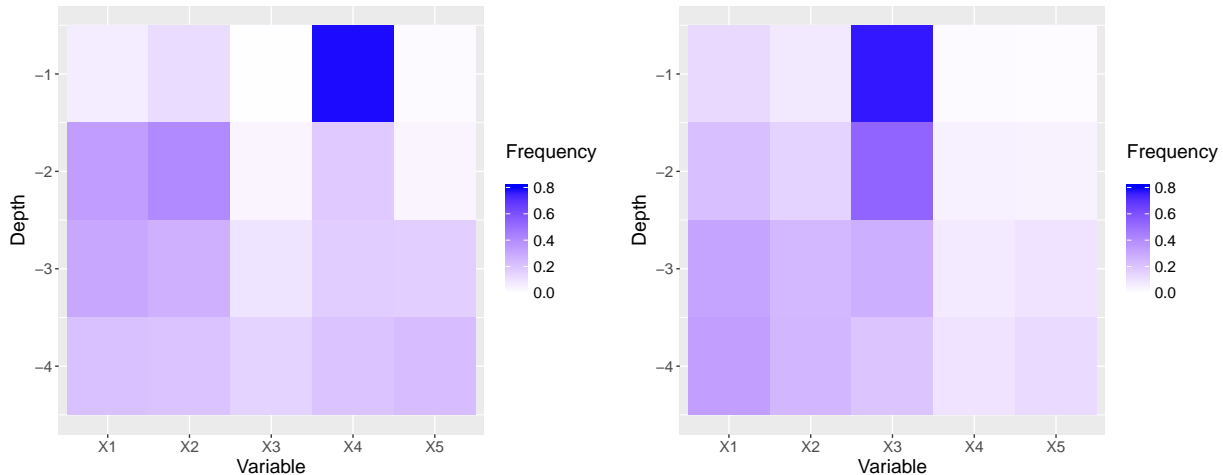


Figure 3: Split frequency plot for CART splits from an honest random forest (left) and residual splits from a local linear forest (right). Each forest was trained on $n = 600$ observations from the data-generating process in 9. Variables 1 through 5 are on the x-axis, and the y-axis gives tree depth, starting with depth 1 at the top of the plot. Tile color is according to split frequency, so variables on which the forest splits frequently at depth j have a dark tile in row j .

for $\varepsilon \sim N(0, \sigma^2)$. This model has become a popular study for evaluating nonparametric regression methods; see for example Chipman et al. [2010] and Taddy et al. [2015]. It is a natural setup to test how well an algorithm handles interactions $\sin(\pi x_1 x_2)$, its ability to pick up a quadratic signal $20(x_3 - 0.5)^2$, and how it simultaneously models strong linear signals $10x_4 + 5x_5$.

Figure 3 displays the split frequencies from an honest random forest (left) using standard CART splits, and a local linear forest (right). The x-axis is indexed by variable, here X_1 through X_5 , and the y-axis gives tree depth for the first 4 levels of tree splits. Tiles are colored according to how often trees in the forest split on that variable; a darker tile denotes more splits at that tree depth. CART splits very frequently on X_4 , which contributes the strongest linear signal, especially at the top of the tree but consistently throughout levels. Local linear forests, on the other hand, rarely split on either of the strong linear signals, instead spending splits on the three that are more difficult to model. In section 4, we show that this indeed corresponds to a performance gain from local linear forests.

2.2 Honest Forests

Unless noted otherwise, all random forests used in this paper are grown using a type of subsample splitting called “honesty,” used by Wager and Athey [2018] to derive the asymptotic distribution of random forest prediction. As outlined in Procedure 1 of Wager and Athey [2018], each tree in an honest forest is grown using two non-overlapping subsamples of the training data, call them \mathcal{I}_b and \mathcal{J}_b . We first choose a tree structure T_b using only the data in \mathcal{J}_b , and write $x \leftrightarrow_b x'$ as the boolean indicator for whether the points x and x' fall into the same leaf of T_b . Then, in a second step, we define the set of neighbors of x as $L_b(x) = \{i \in \mathcal{I}_b : x \leftrightarrow_b X_i\}$; this neighborhood function is what we then use to define the forest weights in (6).

This type of subsample-splitting lets us control for potential overfitting when growing the tree T_b , because the samples \mathcal{J}_b used to define the neighborhood $L_b(x)$ were held out when growing T_b . We note that, despite considerable interest in the literature, there are no available consistency results for random forests with fully grown trees that do not use honesty. Biau [2012] uses a different type of sample splitting, Biau, Devroye, and Lugosi [2008] and Wager and Walther [2015] rely on large leaves, while the results of Scornet, Biau, and Vert [2015] on

fully grown trees rely on an unchecked high-level assumption. Thus, we choose to build our forests with honesty on by default. In our experiments, however, we also consider adaptive (i.e., non-honest) forests as a baseline.

Perhaps the strongest criticism of honesty is that, because of the additional subsample splitting step, we end up with trees grown on less data that are thus less expressive. However, if this is a concern, it is possible to use only a small fraction of the data for the set \mathcal{I}_b , since these samples are used to generate weights and not directly for estimation. By growing a sufficiently large number of trees, we can ensure that the weights are stable. To the extent that concerns about sample size remain, local linear forests appear to be a particularly natural companion to honesty, as we can use the final local regression step to compensate for potential undersmoothing of the raw forests.

2.3 Tuning a Local Linear Forest

We recommend selecting ridge penalties by cross-validation. It is often reasonable to choose different values of λ for forest training and for local linear prediction. During forest growth, equation (8) gives ridge regression coefficients $\hat{\beta}_P$ in each parent leaf. As trees are grown on subsamples of data, over-regularization at this step is a danger even in large leaves. Consequently, small values of λ are advisable for penalization on regressions during forest training. Furthermore, as we move to small leaves, computing meaningful regression coefficients becomes more difficult; the ridge regression can begin to mask signal instead of uncovering it. A heuristic that performs well in practice is to store the regression estimates $\hat{\beta}_P$ on parent leaves P . When the child leaf size shrinks below a cutoff, we use $\hat{\beta}_P$ from the parent node to calculate ridge residual pseudo-outcomes, instead of estimating them from unstable regression coefficients on the small child dataset. In practice, this helps to avoid the pitfalls of over-regularizing and of regressing on a very small dataset when growing the forest. At the final regression prediction step (7), however, a larger ridge penalty can control the variance and better accommodate noisy data.

With increasingly high-dimensional data, feature selection before prediction can significantly reduce error and decrease computation time. Often, a dataset will contain only a small number of features with strong global signals. In other cases, a researcher will know in advance which variables are consistently predictive or of special interest. In these cases, it is reasonable to run the regression prediction step on this smaller subset of predictors expected to contribute overarching trends. Such covariates, if they are not already known, can be chosen by a lasso or another technique for automatic feature selection. Last, it is worth noting that these tuning suggestions are pragmatic in nature; the theoretical guarantees provided in Section 3 are for local linear forests trained without these heuristics.

2.4 Extension to Causal Forests

Finally, although we have focused on local linear regression forests, similar ideas also apply to other types of forests, such as quantile regression forests [Meinshausen, 2006] or, more broadly, generalized random forests [Athey et al., 2018]. Here, we discuss the case of the locally robust causal forests proposed by Athey et al. [2018]; other cases are analogous.

Using notation from Section 1.1, we assume observations (X_i, W_i, Y_i) where W_i is an unconfounded treatment assignment. Locally robust causal forests start by estimating the nuisance components

$$e(x) = \mathbb{P}[W_i = 1 | X_i = x] \text{ and } m(x) = \mathbb{E}[Y_i | X_i = x] \tag{10}$$

using a regression forest, and then estimate the CATE function $\tau(x)$ via a generalized random forest induced by the difference-in-difference estimating equation of Robinson [1988]; see also Nie and Wager [2017] for a broader discussion of this family of CATE estimators. Procedurally,

given a forest kernel $\alpha_i(x)$, a causal forest then estimates the treatment effect as

$$\{\hat{\tau}(x), \hat{a}(x)\} = \operatorname{argmin}_{\tau, a} \left\{ \sum_{i=1}^n \alpha_i(x) \left(Y_i - \hat{m}^{(-i)}(X_i) - a - \tau \left(W_i - \hat{e}^{(-i)}(X_i) \right) \right)^2 \right\}, \quad (11)$$

where the $(-i)$ -superscript denotes leave-one-out predictions from the nuisance models. If nuisance estimates are accurate, the intercept \hat{a} should be 0; however, we leave it in the optimization for robustness.

Local linear causal forests are then a simple generalization of this idea. We first use local linear forests to fit the nuisance components (10), and then add a regularized adjustment to (12),

$$\begin{aligned} \{\hat{\tau}(x), \hat{\theta}_\tau(x), \hat{a}(x), \hat{\theta}_a(x)\} = \operatorname{argmin}_{\tau, \theta} \left\{ \sum_{i=1}^n \alpha_i(x) \left(Y_i - \hat{m}^{(-i)}(X_i) - a - (X_i - x)\theta_a \right. \right. \\ \left. \left. - (\tau + \theta_\tau(X_i - x)) \left(W_i - \hat{e}^{(-i)}(X_i) \right) \right)^2 + \lambda_\tau \|\theta_\tau\|_2^2 + \lambda_a \|\theta_a\|_2^2 \right\}. \end{aligned} \quad (12)$$

We cross-validate local linear causal forests (including λ_τ and λ_a) by minimizing the R -learning criterion recommended by [Nie and Wager \[2017\]](#):

$$\widehat{\operatorname{Err}}(\hat{\tau}(\cdot)) = \sum_{i=1}^n \left(Y_i - \hat{m}^{(-i)}(X_i) - \hat{\tau}(X_i) \left(W_i - \hat{e}^{(-i)}(X_i) \right) \right)^2. \quad (13)$$

3 Asymptotic Theory

Before we delve into the main result and its proof, we briefly discuss why the asymptotic behavior of locally linear forests cannot be directly derived from existing results on regression forests. This is due to a key difference in the dependence structure of the forest. In the regression case, a random forest prediction at x is $\hat{\mu}_{\text{rf}}(x) = \sum_{i=1}^n \alpha_i(x) Y_i$, where, due to honesty, Y_i is independent of $\alpha_i(x)$ given X_i . This conditional independence plays a key role in the argument of [Wager and Athey \[2018\]](#). Analogously to $\hat{\mu}_{\text{rf}}(x)$, we can write the local linear forest prediction as a weighted sum,

$$\hat{\mu}(x) = \sum_{i=1}^n \alpha_i(x) \rho_i, \quad \rho_i = e_1^T M_\lambda^{-1} \begin{pmatrix} 1 \\ X_i - x \end{pmatrix} Y_i, \quad (14)$$

where we use notation Δ, A, J from (7) and define

$$M_\lambda = \Delta^T A \Delta + \lambda J. \quad (15)$$

At a first glance, $\hat{\mu}(x)$ indeed looks like the output of a regression forest trained on observations ρ_i . However, as highlighted in [Figure 4](#), the dependence structure of this object is different. In a random forest, we make Y_i and $\alpha_i(x)$ independent by conditioning on X_i . For a local linear forest, however, conditioning on X_i will not guarantee that ρ_i and $\alpha_i(x)$ are independent, thus breaking a key component in the argument of [Wager and Athey \[2018\]](#).

We now give a Central Limit Theorem for local linear forest predictions, beginning by stating assumptions on the forest.

Assumption 1. (Regular Trees) We assume that the forest grows regular trees: that the trees are symmetric in permutations of training data index, split on every variable with probability bounded from below by $\pi > 0$, and are balanced in that each split puts at least a fraction $\omega > 0$ of parent observations into each child node.

Assumption 2. (Honest Forests) We assume that the forest is honest as described in [Section 2.2](#), meaning that two distinct and independent samples are used to select the splits and estimate parameters in the nodes.

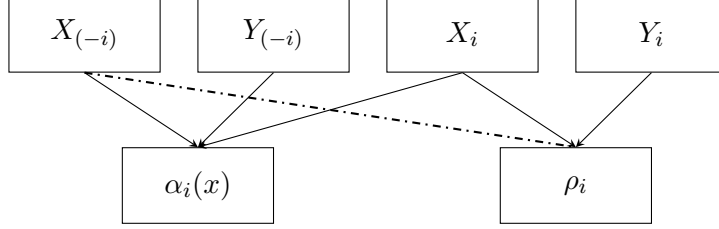


Figure 4: Visualization of the dependence structure in random forests as compared to local linear forests. Arrows indicate a dependence of the derived quantities, weights $\alpha_i(x)$ and pseudo-outcomes ρ_i , on data $X_{(-i)}, X_i, Y_{(-i)}$, and Y_i , where the $(-i)$ -subscript denotes all elements of a vector or matrix except for entry i . The solid lines represent dependencies in both random forests and local linear forests, and the dashed line is a dependence that only exists for local linear forests.

Subsampling plays a central role in our asymptotic theory, as this is what allows us to prove asymptotic normality by building on the work of [Efron and Stein \[1981\]](#). Moreover, subsampling is what we use to tune the bias-variance trade-off of the forest: Forests whose trees are grown on small subsamples have higher bias but lower variance (and vice-versa).

A random forest cannot leverage smoothness, no matter the strength of the assumptions on $\mu(x)$; and this is reflected in existing asymptotic results via conditions on the subsample size. In order to establish asymptotic unbiasedness of forests, [Wager and Athey \[2018\]](#) require a subsample size of at least $n^{\beta_{\text{rf}}}$, with

$$\beta_{\text{rf}} := 1 - \left(1 + \frac{d}{\pi} \frac{\log(\omega^{-1})}{\log((1-\omega)^{-1})} \right)^{-1} < \beta < 1. \quad (16)$$

Here, we show that by using a local regression adjustment and assuming smoothness of $\mu(\cdot)$, we can grow trees on smaller subsamples of size (17) without incurring asymptotic bias. This allows us to decrease the variance (and improve the accuracy) of our estimates.

Our main result establishes asymptotic normality of local linear forest predictions, and gives this improved subsampling rate.

Theorem 1. *Suppose we have training data $Z_i = (X_i, Y_i)$ identically and independently distributed on $[0, 1]^d \times \mathbb{R}$, where the density of X_i is bounded away from infinity. Suppose furthermore that $\mu(x) = \mathbb{E}[Y | X = x]$ is twice continuously differentiable, with a uniformly bounded second derivative, and that $\text{Var}[Y | X = x] > 0$. Last, say that our trees are grown according to Assumptions 1 and 2, with subsamples of size s with $s = n^\beta$, for*

$$\beta_{\min} := 1 - \left(1 + \frac{d}{1.56\pi} \frac{\log(\omega^{-1})}{\log((1-\omega)^{-1})} \right)^{-1} < \beta < 1. \quad (17)$$

Then there is a sequence $\sigma_n(x) \rightarrow 0$ such that

$$\frac{\hat{\mu}_n(x) - \mu(x)}{\sigma_n(x)} \Rightarrow N(0, 1), \quad \sigma_n^2(x) = O(n^{-(1-\beta)})$$

We begin by decomposing $\hat{\mu}(x)$ into bias $\delta_1(x)$ and variance $\hat{\gamma}_n(x)$, the latter of which we will approximate by a generalized random forest. Thanks to our assumed uniform bound on the second derivative of $\mu(\cdot)$, a Taylor expansion of $Y_i = \mu(X_i) + \varepsilon_i$ around $\mu(x)$ yields the following decomposition,

$$\hat{\mu}(x) = \sum_{i=1}^n e_1^T M_\lambda^{-1} \begin{pmatrix} 1 \\ X_i - x \end{pmatrix} \alpha_i Y_i = \mu(x) + \delta_1(x) + \hat{\gamma}_n(x) + O(\bar{R}^2), \quad (18)$$

where \bar{R}^2 is the average squared radius of leaves T_b in the forest, and we have isolated the two error terms

$$\delta_1(x) = \sum_{i=1}^n \alpha_i(x) e_1^T M_\lambda^{-1} \begin{pmatrix} 1 \\ X_i - x \end{pmatrix} \nabla \mu(x)^T \begin{pmatrix} 0 \\ X_i - x \end{pmatrix}, \quad (19)$$

$$\hat{\gamma}_n(x) = \sum_{i=1}^n \alpha_i(x) e_1^T M_\lambda^{-1} \begin{pmatrix} 1 \\ X_i - x \end{pmatrix} \varepsilon_i. \quad (20)$$

Here the diameter (and corresponding radius) of a tree leaf is the length of the longest line segment that can fit completely inside of the leaf.

To control the radius R_{T_b} of a typical leaf containing x (and thus the Taylor error in (18)), we use the following bound. Suppose $X_1, \dots, X_s \sim U([0, 1]^d)$ independently, and let T_b be any regular, random-split tree and let $R_{T_b}(x)$ be the radius of its leaf containing the test point x . Then Lemma 2 of [Wager and Athey \[2018\]](#) implies that,

$$\mathbb{P}(R_{T_b}^2(x) \geq r_s) \leq d \left(\frac{s}{2k-1} \right)^{-\frac{\eta^2}{2} \frac{1}{\log(\omega^{-1})} \frac{\pi}{d}}, \quad (21)$$

$$\text{where } r_s = \sqrt{d} \left(\frac{s}{2k-1} \right)^{-1.98(1-\eta) \frac{\log((1-\omega)^{-1})}{\log(\omega^{-1})} \frac{\pi}{d}},$$

for any $0 < \eta < 1$ and for sufficiently large s .

Next, to control the behavior of $\hat{\gamma}_n(x)$, we show that M_λ concentrates around its expectation. The proof of Lemma 2 uses concentration bounds for U -statistics given by [Hoeffding \[1963\]](#).

Lemma 2. *Let X_1, \dots, X_n be independent and identically distributed on $[0, 1]^d$. Let $\alpha_1(x), \dots, \alpha_n(x)$ be forest weights from trees grown on subsamples of size s and radius bounded by r_s from (21). Then,*

$$\|M_\lambda - \mathbb{E}[M_\lambda]\|_\infty = \mathcal{O}_P\left(r_s^2 \sqrt{s/n}\right)$$

Lemma 2 enables coupling $\hat{\gamma}_n$ with an approximation $\tilde{\gamma}_n$, defined as

$$\tilde{\gamma}_n(x) = \sum_{i=1}^n \alpha_i \tilde{Y}_i, \quad \text{where } \tilde{Y}_i = e_1^T \mathbb{E}[M_\lambda]^{-1} \begin{pmatrix} 1 \\ X_i - x \end{pmatrix} \varepsilon_i.$$

Now, \tilde{Y}_i is independent of $\alpha_i(x)$ conditionally on X_i (because the problematic associations in Figure 4 were mediated by M_λ), and consequently $\tilde{\gamma}_n$ can be characterized via standard tools used to study random forests.

Corollary 3. *Under the conditions from Lemma 2, $\hat{\gamma}_n(x)$ and $\tilde{\gamma}_n(x)$ are coupled at the following rate.*

$$|\hat{\gamma}_n(x) - \tilde{\gamma}_n(x)| = \mathcal{O}_P\left(\lambda^{-1} r_s^2 \sqrt{s/n}\right)$$

Corollary 3 dictates our choice of λ at $\mathcal{O}(r_s^2 \sqrt{s/n})$. For any $\lambda < \mathcal{O}(r_s^2 \sqrt{s/n})$, $|\hat{\gamma}_n(x) - \tilde{\gamma}_n(x)|$ may not converge to 0. On the other hand, observe that letting $\lambda \rightarrow \infty$ will make local linear forest predictions equivalent to generalized random forest predictions. An appropriate choice of λ allows us to derive the improved asymptotic normality of $\tilde{\gamma}_n(x)$, given below in Lemma 4.

Lemma 4. *Suppose that trees T are honest, regular, and grown on subsamples of size s , with $s = n^\beta$ for some*

$$\beta > 1 - \left(1 + \frac{1}{1.56} \frac{\log(\omega^{-1})}{\log((1-\omega)^{-1})} \frac{d}{\pi}\right)^{-1} = \beta_{\min}$$

where π and ω are constants defined in the forest assumptions. Suppose further that observations X_1, \dots, X_n are i.i.d. on $[0, 1]^d$ with a density f bounded away from infinity, and that the

conditional mean function $\mu(x)$ is twice Lipschitz continuous at x . Last, suppose we choose $\lambda = \mathcal{O}(r_s^2 \sqrt{s/n})$. Then there is a sequence $\sigma_n(x) \rightarrow 0$ such that

$$\frac{\tilde{\gamma}_n(x)}{\sigma_n(x)} \Rightarrow \mathcal{N}(0, 1)$$

Refer back to the Taylor decomposition given in (18). Lemma 4 gives the asymptotic distribution of $\tilde{\gamma}_n(x)$, and the corresponding variance $\sigma_n^2(x)$. Lemma 5 provides a complementary result, controlling $\delta_1(x)$.

Lemma 5. *Let X_1, \dots, X_n be independent and identically distributed on $[0, 1]^d$. Suppose the conditional mean function $\mu(x) = \mathbb{E}[Y | X = x]$ is twice Lipschitz continuous, and let $\hat{\mu}_n(x)$ be the local linear forest estimate at x . Last, suppose we choose*

$$\lambda = \mathcal{O}(r_s^2 \sqrt{s/n})$$

Then,

$$\delta_1(x) = \mathcal{O}\left(n^{-\beta \cdot 0.78 \frac{\log((1-\omega)^{-1})}{\log(\omega^{-1})} \frac{\pi}{d}} n^{(\beta-1)/4}\right)$$

3.1 Proof of Theorem 1

Recall the decomposition in equation (18),

$$\hat{\mu}(x) = \mu(x) + \delta_1(x) + \hat{\gamma}_n(x).$$

Lemma 4 gives the distribution of $\tilde{\gamma}_n(x)$ for sufficiently large n , with asymptotic variance $\sigma_n^2(x)$. Corollary 3 establishes the coupling between $\hat{\gamma}_n(x)$ and $\tilde{\gamma}_n(x)$ at rate $\mathcal{O}_P(\lambda^{-1} r_s^2 \sqrt{s/n})$. From these two results, we know there exists $\sigma_n(x) \rightarrow 0$ such that

$$\frac{\hat{\gamma}_n(x)}{\sigma_n(x)} \Rightarrow \mathcal{N}(0, 1).$$

From Lemma 5, for any $\varepsilon > 0$,

$$\begin{aligned} \frac{\delta_1(x)}{\sigma_n(x)} &= \mathcal{O}\left(n^{\frac{1}{2}\left(-\beta \cdot 0.78 \frac{\log((1-\omega)^{-1})}{\log(\omega^{-1})} \frac{\pi}{d}\right)} n^{\frac{1}{2}(\beta-1)} n^{\frac{1}{2}(1+\varepsilon-\beta)}\right) \\ &= \mathcal{O}\left(n^{\frac{1}{2}\left(\varepsilon-\beta\left(0.78 \frac{\log((1-\omega)^{-1})}{\log(\omega^{-1})} \frac{\pi}{d}\right)\right)}\right) \end{aligned}$$

Clearly for sufficiently small ε and $\beta > \beta_{\min}$, we have $\delta_1(x)/\sigma_n(x) = o_p(1)$. Therefore, as $n, s \rightarrow \infty$ appropriately, Slutsky's Lemma implies that $(\hat{\mu}_n(x) - \mu(x))/\sigma_n(x) \Rightarrow \mathcal{N}(0, 1)$.

4 Simulation Study

4.1 Methods

In this section, we compare local linear forests, (honest) random forests, adaptive (i.e., non-honest) random forests, and BART [Chipman et al., 2010]. We also include a lasso-random forest baseline for local linear forests, proceeding as follows. Split the data and on the first half, train a lasso [Tibshirani, 1996] regression; on the second half, use a random forest to model the residuals. Like local linear forests, this method combines regression and forests and uses them to model different signals in the data, making it a natural comparison.

Local linear forests are tuned via 10-fold cross validation, with tuning parameters `mtry` (number of splitting variables), minimum leaf size, sample fraction used in each tree, and regularization for splitting and prediction. Variables for the regression at prediction are selected via

	Lasso-RF (cv)	BART	RF	RF (cv)	LLF	LLF (cv)
$d = 5$	1.94	34.6	0.39	1.59	0.59	4.05
$d = 50$	3.53	42.8	1.17	3.51	1.11	7.51

Table 2: Average runtime in seconds for each method on data generated from equation 9. In these simulations, to mirror the setup we use to evaluate RMSE, we fix training size $n = 600$, hold $\sigma = 5$ and predict on 1000 test points. For local linear forests and random forests, we report both the runtime with pre-fixed parameters and the runtime with cross-validation (cv). Random forests with cross-validation are regression forests from `grf` with automatic self-tuning; both random forests included are honest. We report the runtime for each method averaged over 50 runs.

the lasso after splitting the data. Random forests are run using `grf` [Tibshirani et al., 2018] with honesty, and are cross-validated via the default cross-validation routine in `grf`, which selects values for `mtry`, minimum leaf size, sample fraction, and two parameters (alpha and imbalance penalty) that control split balance. Adaptive (i.e., non-honest) random forests are also fit via the `grf` package, with honesty set to `FALSE`, and are cross-validated equivalently. Lasso is implemented via `glmnet` [Friedman et al., 2010] and is cross-validated with their automatic cross-validation feature. The random forests we train on the lasso residuals are adaptive random forests cross-validated as before.

BART for treatment effect estimation is implemented following Hill [2011]. As is standard, we use the `BayesTree` package [Chipman and McCulloch, 2016] without any additional tuning. The motivation for not tuning is that, first, if we want to interpret the BART posterior in a Bayesian sense (as is often done), then cross-validating on the prior is hard to justify, and in fact most existing papers do not cross-validate BART. Second, BART is much slower than the other methods we consider, and cross-validation would make it prohibitively slow. For example, Table 2 displays the average runtime (in seconds) of this process for local linear forests (with fixed parameters and with cross-validation), random forests (with the same), lasso, and BART, on the example (9) with sample size $n = 600$, error standard deviation $\sigma = 1$, and dimension at $d = 5$ and $d = 50$. We can see that even without cross-validation, BART has by far the longest runtime of the peer methods.

4.2 Simulation Design

The first design we study is Friedman’s example from equation (9). We generate X_1, \dots, X_n i.i.d. $U[0, 1]^d$ and simulate responses

$$y = 10 \sin(\pi x_1 x_2) + 20(x_3 - 0.5)^2 + 10x_4 + 5x_5 + \epsilon, \quad \epsilon \sim N(0, \sigma^2)$$

We calculate root mean-squared error (RMSE) on 1000 test points, averaged over 50 runs. Figure 5 shows errors at $n = 600$ fixed, with dimension d varying from 10 to 50. There are two plots shown, to highlight the differences between error variance $\sigma = 5$ and $\sigma = 20$. Table 3 reports a grid of errors for dimensions 10, 30, and 50, with $n = 600$ and 1000, and σ taking values of 1, 5, 10, and 20.

The second design we consider is given in Section 1. We simulate X_1, \dots, X_n i.i.d. $U[-1, 1]^d$ and model responses as in equation (1),

$$y = \log(1 + e^{6x_1}) + \epsilon, \quad \epsilon \sim N(0, \sigma^2)$$

Again we test on a grid, letting dimension d take values in 5, 10, and 20, n either 600 or 1000, and σ at 0.1, 1, and 2. We calculate RMSE over 50 runs on 1000 test points. Errors are reported in Table 4.

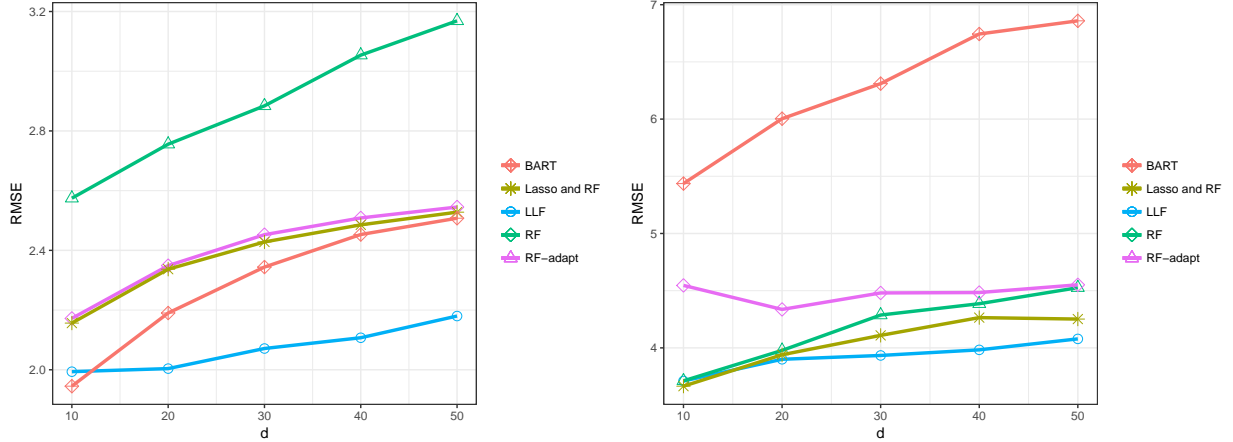


Figure 5: RMSE of predictions on 1000 test samples from equation 9, with $n = 600$ held fixed and dimension d varied from 10 to 50. Plots are shown for error standard deviation $\sigma = 5$ (left) and $\sigma = 20$ (right). Error was calculated in increments of 10, and averaged over 50 runs per method at each step. Methods evaluated are (honest) random forests (RF), local linear forests (LLF), adaptive random forests (RF-adapt), lasso, and BART.

4.3 Results

Figure 5 shows RMSE from equation 9 at $\sigma = 5$ (left) and $\sigma = 20$ (right). In Section 2, we showed that local linear forests and standard regression forests split on very different variables when generating weights. Our intuition is that these are splits we have saved; we model the strong linear effects at the end with the local regression, and use the forest splits to capture more nuanced local relationships for the weights. Local linear forests consistently perform well as we vary the parameters data-generating process, lending this credibility.

The lasso-random forest baseline lines up closely with adaptive random forests in the low-noise case; in the high-noise case, it aligns more closely with local linear forests, albeit with larger errors. BART, which does quite well in low-noise problems, suffers significantly when we decrease the signal-to-noise ratio as we do in this simulation. Note also that random forests suffer in the lower-noise case, but move to outperform in the high noise case. As we only have $n = 600$ training points, and growing honest trees forces further subsampling, we have designed a difficult simulation for this method. Removing the honesty constraint and growing original random forests helps to improve RMSE, but adding the local linear correction lets us improve RMSE more while retaining honesty. Table 3 shows the fuller RMSE comparison from Friedman’s model.

We move to the second simulation setup, equation 1, meant to evaluate how methods perform in cases with a strong linear trend in the mean. Tree-based methods will be prone to bias on this setup, as the forests cannot always split on x_1 , and because the signal is global and smooth. Table 4 gives RMSE. Local linear forests do quite well here; they detect the strong linear signal in the tail, as we saw in Figure 1, and model it successfully throughout the range of the feature space.

4.4 Local Linear Causal Forests

In Section 1.1, we introduced a real-data example where the local linear extension of causal forests naturally applies. Evaluating errors empirically, however, is difficult, so we supplement that with a simulation also used by Wager and Athey [2018] in evaluating causal forests and Künzel et al. [2017], used to evaluate their meta-learner called the X-learner. Here we let $X \sim U([0, 1]^d)$. We fix the propensity $e(x) = 0.5$ and $\mu(x) = 0$, and generate a causal effect τ

p	n	σ	Lasso-RF	BART	RF	RF-adapt	LLF
10	600	1	1.69	0.816	2.21	1.83	1.64
10	1000	1	1.45	0.647	1.95	1.59	1.35
30	600	1	1.91	0.990	2.49	2.05	1.68
30	1000	1	1.64	0.78	2.19	1.86	1.57
50	600	1	2.00	1.21	2.62	2.12	1.85
50	1000	1	1.70	0.842	2.48	2.00	1.71
10	600	5	2.17	1.92	2.54	2.15	1.93
10	1000	5	1.96	1.70	2.31	2.02	1.80
30	600	5	2.43	2.44	2.86	2.48	2.02
30	1000	5	2.25	2.01	2.57	2.20	1.92
50	600	5	2.53	2.51	3.12	2.60	2.08
50	1000	5	2.34	2.24	2.79	2.27	2.04
10	600	10	2.62	3.04	2.96	2.86	2.56
10	1000	10	2.32	2.78	2.74	2.62	2.28
30	600	10	3.01	3.60	3.49	3.17	2.62
30	1000	10	2.64	3.42	2.95	2.90	2.35
50	600	10	3.24	3.87	3.78	3.24	2.65
50	1000	10	2.82	3.57	3.50	2.90	2.36
10	600	20	3.67	5.34	3.72	4.66	3.71
10	1000	20	3.18	4.92	3.29	4.08	3.46
30	600	20	4.11	5.92	4.28	4.46	3.93
30	1000	20	3.62	5.79	4.15	3.96	3.07
50	600	20	4.26	6.67	4.52	4.59	4.08
50	1000	20	3.87	6.19	4.60	4.22	3.80

Table 3: RMSE from simulations on equation 9. We vary the dimension p from 10 to 50 predictors in increments of 20, and consider error standard deviation σ ranging from 1 to 20, for a variety of signal-to-noise ratios. Note that for this setting, $\text{Var}(\mathbb{E}[Y | X]) \approx 23.8$, as approximated over 10,000 Monte Carlo repetitions; so letting $\sigma = 1$ corresponds to a signal-to-noise ratio of about 23.8, while letting $\sigma = 20$ corresponds to a signal-to-noise ratio of about 0.24. We train on $n = 600$ and $n = 1000$ points, and report test errors from predicting on 1000 test points. All errors reported are averaged over 50 runs and the methods are cross-validated as described in Section 4.1. Minimizing errors are reported in bold.

from each

$$\tau(x) = \zeta(x_1)\zeta(x_2), \quad \zeta(x) = \frac{2}{1 + e^{-20(x-1/3)}} \quad (22)$$

$$\tau(x) = \zeta(x_1)\zeta(x_2), \quad \zeta(x) = 1 + \frac{1}{1 + e^{-20(x-1/3)}} \quad (23)$$

We will assume unconfoundedness [Rosenbaum and Rubin, 1983]; therefore, because we hold propensity fixed, this is a randomized controlled trial.

We compare local linear forests, causal forests, and X-BART, which is the X-learner using BART as a base-learner. Causal forests as implemented by `grf` are tuned via the automatic self-tuning feature, as were the regression forests used earlier in this simulation study. As X-BART is a BART method, we do not cross-validate (note that the authors recommend X-BART specifically for when a user does not want to carefully tune), and we acknowledge that this may hinder its performance. Local linear causal forests are tuned via cross-validation as described in 2.4.

We consider relatively small sample sizes ranging from $n = 400$ to $n = 1200$ with dimension $d = 20$, to see how effectively we can learn a smooth heterogeneous treatment effect in the

p	n	σ	Lasso-RF	BART	RF	RF-adapt	LLF
5	600	0.1	0.0972	0.0713	0.101	0.476	0.0544
5	1000	0.1	0.0701	0.0559	0.0845	0.398	0.0450
10	600	0.1	0.128	0.0762	0.115	0.310	0.0711
10	1000	0.1	0.0917	0.0585	0.144	0.249	0.0875
20	600	0.1	0.141	0.0810	0.142	0.319	0.0870
20	1000	0.1	0.0986	0.0622	0.162	0.256	0.101
5	600	1	0.267	0.272	0.208	0.502	0.160
5	1000	1	0.216	0.247	0.183	0.433	0.136
10	600	1	0.304	0.362	0.230	0.388	0.160
10	1000	1	0.262	0.323	0.212	0.325	0.149
20	600	1	0.344	0.405	0.221	0.388	0.161
20	1000	1	0.271	0.352	0.214	0.323	0.146
5	600	2	0.457	0.527	0.324	0.630	0.271
5	1000	2	0.386	0.496	0.290	0.563	0.230
10	600	2	0.505	0.606	0.350	0.538	0.272
10	1000	2	0.417	0.548	0.302	0.480	0.235
20	600	2	0.559	0.687	0.380	0.533	0.272
20	1000	2	0.454	0.607	0.308	0.461	0.243

Table 4: RMSE from simulations on equation 1 on local linear forests, random forests, adaptive (non-honest) random forests, lasso-random forest, and BART. We vary sample size n , error variance σ , and ambient dimension p , and report test error on 1000 test points. We estimate $\text{Var}[\mathbb{E}[Y | X]]$ as 3.52 over 10,000 Monte Carlo repetitions, so that signal-to-noise ratio ranges from 352 at $\sigma = 0.1$ to 0.88 at $\sigma = 2$. All errors are averaged over 50 runs, and minimizing errors are in bold.

presence of many noise covariates. RMSE over 100 repetitions is reported in Table 5. Wager and Athey [2018] point to Simulation 1 (equation 22) especially as a simulation that highlights how forests can suffer on the boundary of a feature space, because there is a spike near $x = 0$. We can see that in this simulations, local linear forests, which do not suffer from this boundary bias, give a significant improvement over causal forests. Both of these setups, however, are reasonable tests for how a method can learn heterogeneity, and demonstrate how we can improve with thoughtful variable selection and robustness to smooth heterogeneous signals.

4.5 The Value of Local Linear Splitting

We close this section with an experiment that highlights the benefit of the splitting rule proposed in Section 2.1. We generate X_1, \dots, X_n independently and uniformly over $[0, 1]^d$. We keep a cubic signal $20(x_1 - 0.5)^3$ constant across simulations, and on each run we increase the dimension and add another linear signal. Let $\xi_j = \mathbb{1}\{d \leq j\}$ and generate responses

$$y = 20(x_1 - 0.5)^3 \xi_1 + \sum_{j=2}^3 10x_j \xi_j + \sum_{j=4}^5 5x_j \xi_j + \sum_{j=6}^{20} 2x_j \xi_j \quad (24)$$

For example, at simulation 3 we have $\xi_1, \xi_2, \xi_3 = 1$ and hence we model $y = 20(x_1 - 0.5)^3 + 10x_2 + 10x_3$. RMSE is displayed in Figure 6.

In low dimension and with few linear signals, all three methods are comparable. However, they begin to differ quickly. Random forests are not designed for models with so many global linear signals, and hence their RMSE increases dramatically with d . Moreover, as we add more linear effects, the gap between the two candidate splitting rules grows; heuristically, it becomes more important not to waste splits. The more signal we can model in a regression, the more

n	Simulation 1 (equation 22)			Simulation 2 (equation 23)		
	X-BART	CF	LLCF	X-BART	CF	LLCF
200	0.864	0.834	0.673	0.694	0.737	0.601
400	0.495	0.619	0.471	0.585	0.466	0.420
600	0.451	0.592	0.423	0.504	0.379	0.337
800	0.437	0.577	0.412	0.481	0.350	0.331
1000	0.354	0.463	0.325	0.480	0.347	0.314
1200	0.290	0.379	0.280	0.417	0.261	0.257

Table 5: Average RMSE of predicting the heterogeneous treatment effect τ_i on 100 repetitions of the simulation given in equation (22). We vary the sample size n from 200 to 1200 in increments of 200, always testing on 2000 test points. We report errors from local linear causal forests (LLCF), causal forests (CF), and the X-learner with BART as base learner (X-BART). Minimizing errors are reported in bold.

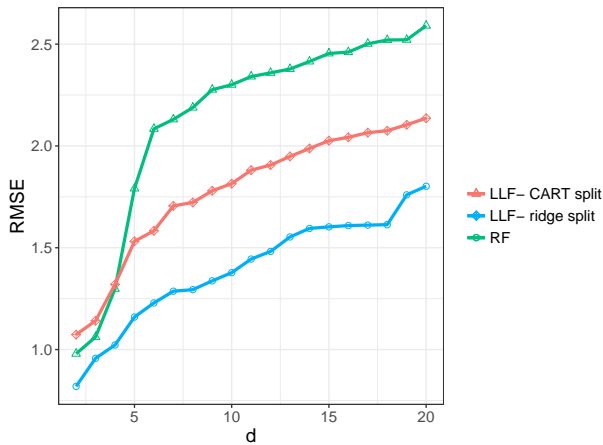


Figure 6: Results from testing different splitting rules on data generated from equation 24. Here the x-axis is dimension d , varying from 2 to 20, and we plot the RMSE of prediction from random forests and from local linear forests with CART splits and with the ridge residual splits. We let $n = 600$ and check results on 600 test points at 50 runs for each value of d .

benefit we get from the residual splitting rule. Note that at a certain point, however, the gap between splitting rules stays constant. Once we simply cannot fit a more complex linear function with a fixed amount of data, the marginal benefits of the residual splitting rule level out. We show this to emphasize the contexts in which this splitting rule meaningfully affects the results.

5 Discussion

In this paper, we proposed local linear forests as a modification of random forests equipped to model smooth signals and fix boundary bias issues. We presented asymptotic theory showing that, if we can assume smoother signals, we can get better rates of convergence than standard random forests. We showed on the welfare dataset that local linear forests can effectively model smooth heterogeneous causal effects, and illustrated in several simulations when and why they out-perform competing methods.

There remains room for meaningful future work on this topic. In some applications, we may be interested in estimating the slope parameter $\theta(x)$, rather than just crudely accounting for it to improve the precision of $\mu(x)$. While local linear forests may be an appropriate method

for doing so, we have not yet explored this topic and think it could be of significant interest. Furthermore, we expect that confidence intervals from generalized random forests will apply to local linear forests, but may be able to get some improvements; this is another worthwhile direction for future research.

References

- Alberto Abadie and Guido W Imbens. Bias-corrected matching estimators for average treatment effects. *Journal of Business & Economic Statistics*, 29(1):1–11, 2011.
- Yali Amit and Donald Geman. Shape quantization and recognition with randomized trees. *Neural Comput.*, 9(7):1545–1588, October 1997. ISSN 0899-7667. doi: 10.1162/neco.1997.9.7.1545.
- Susan Athey and Guido W Imbens. Machine learning methods for estimating heterogeneous causal effects. *stat*, 1050(5), 2015.
- Susan Athey, Julie Tibshirani, and Stefan Wager. Generalized random forests. *Annals of Statistics*, forthcoming, 2018.
- G erard Biau. Analysis of a random forests model. *J. Mach. Learn. Res.*, 13(1):1063–1095, April 2012. ISSN 1532-4435.
- G erard Biau, Luc Devroye, and G abor Lugosi. Consistency of random forests and other averaging classifiers. *JMLR*, 9:2015–2033, 2008.
- L. Breiman, J. Friedman, C.J. Stone, and R.A. Olshen. *Classification and Regression Trees*. The Wadsworth and Brooks-Cole statistics-probability series. Taylor & Francis, 1984. ISBN 9780412048418.
- Leo Breiman. Bagging predictors. *Mach. Learn.*, 24(2):123–140, August 1996. ISSN 0885-6125. doi: 10.1023/A:1018054314350.
- Leo Breiman. Random forests. *Machine Learning*, 45(1):5–32, Oct 2001. ISSN 1573-0565. doi: 10.1023/A:1010933404324.
- Peter B uhlmann and Bin Yu. Analyzing bagging. *The Annals of Statistics*, 30(4):927–961, 2002.
- Ming-Yen Cheng, Jianqing Fan, and J. S. Marron. On automatic boundary corrections. *The Annals of Statistics*, 25(4):1691–1708, 1997. ISSN 00905364.
- Hugh Chipman and Robert McCulloch. *BayesTree: Bayesian Additive Regression Trees*, 2016. URL <https://CRAN.R-project.org/package=BayesTree>. R package version 0.3-1.4.
- Hugh A. Chipman, Edward I. George, and Robert E. McCulloch. Bart: Bayesian additive regression trees. *Ann. Appl. Stat.*, 4(1):266–298, 03 2010. doi: 10.1214/09-AOAS285.
- William S. Cleveland. Robust locally weighted regression and smoothing scatterplots. *Journal of the American Statistical Association*, 74:829–836, 1979.
- William S. Cleveland and Susan J. Devlin. Locally weighted regression: An approach to regression analysis by local fitting. *Journal of the American Statistical Association*, 83(403):596–610, 1988. doi: 10.1080/01621459.1988.10478639.
- D Richard Cutler, Thomas C Edwards Jr, Karen H Beard, Adele Cutler, Kyle T Hess, Jacob Gibson, and Joshua J Lawler. Random forests for classification in ecology. *Ecology*, 88(11):2783–2792, 2007.

- Ramón Díaz-Uriarte and Sara Alvarez De Andres. Gene selection and classification of microarray data using random forest. *BMC bioinformatics*, 7(1):3, 2006.
- Bradley Efron and Charles Stein. The jackknife estimate of variance. *The Annals of Statistics*, pages 586–596, 1981.
- Jianqing Fan and Irene Gijbels. Variable bandwidth and local linear regression smoothers. *Ann. Statist.*, 20(4):2008–2036, 12 1992. doi: 10.1214/aos/1176348900.
- Jianqing Fan and Irne Gijbels. *Local polynomial modelling and its applications*. Number 66 in Monographs on statistics and applied probability series. Chapman & Hall, London [u.a.], 1996. ISBN 0412983214.
- Jerome Friedman, Trevor Hastie, and Robert Tibshirani. Regularization paths for generalized linear models via coordinate descent. *Journal of Statistical Software*, 33(1):1–22, 2010. URL <http://www.jstatsoft.org/v33/i01/>.
- Jerome H. Friedman. Multivariate adaptive regression splines. *Ann. Statist.*, 19(1):1–67, 03 1991. doi: 10.1214/aos/1176347963.
- Donald P. Green and Holger L. Kern. Modeling heterogeneous treatment effects in survey experiments with bayesian additive regression trees. *Public Opinion Quarterly*, 76(3):491–511, 2012. doi: 10.1093/poq/nfs036.
- James J Heckman, Hidehiko Ichimura, and Petra Todd. Matching as an econometric evaluation estimator. *The review of economic studies*, 65(2):261–294, 1998.
- Jennifer L Hill. Bayesian nonparametric modeling for causal inference. *Journal of Computational and Graphical Statistics*, 20(1):217–240, 2011.
- Wassily Hoeffding. Probability inequalities for sums of bounded random variables. *American Statistical Association Journal*, March 1963.
- Torsten Hothorn, Berthold Lausen, Axel Benner, and Martin Radespiel-Troger. Bagging survival trees. *Statistics in Medicine*, 23:77–91, 2004.
- Guido W Imbens and Donald B Rubin. *Causal inference in statistics, social, and biomedical sciences*. Cambridge University Press, 2015.
- Soren R. Künnel, Jasjeet S. Sekhon, Peter J. Bickel, and Bin Yu. Meta-learners for Estimating Heterogeneous Treatment Effects using Machine Learning. *ArXiv e-prints*, June 2017.
- Yehua Li and Tailen Hsing. Uniform convergence rates for nonparametric regression and principal component analysis in functional/longitudinal data. *Ann. Statist.*, 38(6):3321–3351, 12 2010. doi: 10.1214/10-AOS813.
- Catherine Loader. *locfit: Local Regression, Likelihood and Density Estimation.*, 2013. URL <https://CRAN.R-project.org/package=locfit>. R package version 1.5-9.1.
- Clive Loader. *Local regression and likelihood*. New York: Springer-Verlag, 1999. ISBN 0-387-9877.
- Nicolai Meinshausen. Quantile regression forests. *Journal of Machine Learning Research*, 7 (Jun):983–999, 2006.
- Lucas Mentch and Giles Hooker. Quantifying uncertainty in random forests via confidence intervals and hypothesis tests. *J. Mach. Learn. Res.*, 17(1):841–881, January 2016. ISSN 1532-4435.

- Whitney K. Newey. Kernel estimation of partial means and a general variance estimator. *Econometric Theory*, 10(2):233–253, 1994. ISSN 02664666, 14694360.
- Xinkun Nie and Stefan Wager. Learning objectives for treatment effect estimation. *arXiv preprint arXiv:1712.04912*, 2017.
- R Core Team. *R: A Language and Environment for Statistical Computing*. R Foundation for Statistical Computing, Vienna, Austria, 2018. URL <https://www.R-project.org/>.
- Peter M Robinson. Root-n-consistent semiparametric regression. *Econometrica: Journal of the Econometric Society*, pages 931–954, 1988.
- Paul R. Rosenbaum and Donald B. Rubin. The central role of the propensity score in observational studies for causal effects. *Biometrika*, 70(1):41–55, 1983. doi: 10.1093/biomet/70.1.41.
- Erwan Scornet, Grard Biau, and Jean-Philippe Vert. Consistency of random forests. *Ann. Statist.*, 43(4):1716–1741, 08 2015. doi: 10.1214/15-AOS1321.
- Charles J. Stone. Consistent nonparametric regression. *The Annals of Statistics*, 5:595–620, 1977.
- Vladimir Svetnik, Andy Liaw, Christopher Tong, J Christopher Culberson, Robert P Sheridan, and Bradley P Feuston. Random forest: a classification and regression tool for compound classification and QSAR modeling. *Journal of Chemical Information and Computer Sciences*, 43(6):1947–1958, 2003.
- M. Taddy, C.-S. Chen, J. Yu, and M. Wyle. Bayesian and empirical Bayesian forests. *ArXiv e-prints*, feb 2015.
- Julie Tibshirani, Susan Athey, Stefan Wager, Marvin Wright, and all contributors to the included version of Eigen. *grf: Generalized Random Forests (Beta)*, 2018. URL <https://github.com/swager/grf>. R package version 0.9.3.
- Robert Tibshirani. Regression shrinkage and selection via the lasso. *Journal of the Royal Statistical Society, Series B*, 58:267–288, 1996.
- Robert Tibshirani and Trevor Hastie. Local likelihood estimation. *Journal of the American Statistical Association*, 82(398):559–567, 1987.
- Stefan Wager and Susan Athey. Estimation and inference of heterogeneous treatment effects using random forests. *Journal of the American Statistical Association*, forthcoming, 2018.
- Stefan Wager and Guenther Walther. Adaptive concentration of regression trees, with application to random forests. *arXiv preprint arXiv:1503.06388*, 2015.
- Stefan Wager, Trevor Hastie, and Bradley Efron. Confidence intervals for random forests: The jackknife and the infinitesimal jackknife. *J. Mach. Learn. Res.*, 15(1):1625–1651, January 2014. ISSN 1532-4435.
- Fang Yao, Hans-Georg Muller, and Jane-Ling Wang. Functional linear regression analysis for longitudinal data. *Ann. Statist.*, 33(6):2873–2903, 12 2005. doi: 10.1214/009053605000000660.
- Yichen Zhou and Giles Hooker. Boulevard: Regularized stochastic gradient boosted trees and their limiting distribution. *arXiv preprint arXiv:1806.09762*, 2018.
- Ruoqing Zhu, Donglin Zeng, and Michael R Kosorok. Reinforcement learning trees. *Journal of the American Statistical Association*, 110(512):1770–1784, 2015.

Appendix: Remaining Proofs

Here we give the proofs remaining from Section 3. We begin with Lemma 6, which gives a bound on the bias of $\hat{\gamma}_n(x)$.

Coupling between $\hat{\gamma}_n(x)$ and $\tilde{\gamma}_n(x)$

Lemma 6. *Suppose we have training data $(X_1, Y_1), \dots, (X_n, Y_n)$ with X_1, \dots, X_n i.i.d. $[0, 1]^d$ and $\gamma(x) = \mathbb{E}[Y \mid X = x]$ twice Lipschitz continuous. Assume further that we have a forest grown on honest, regular trees T , and all conditions of Lemma 2 from [Wager and Athey \[2018\]](#) hold. Then, for $\omega \leq 0.2$, the bias of the random forest prediction $\hat{\gamma}(x)$ is bounded by*

$$|\mathbb{E}[\hat{\gamma}(x)] - \gamma(x)| = \mathcal{O}\left(s^{-0.78 \frac{\log((1-\omega)^{-1})}{\log(\omega^{-1})} \frac{\pi}{d}}\right)$$

Proof. We begin with two observations. First by assuming the conditional mean function is twice Lipschitz continuous, and second by honesty, we have

$$\begin{aligned} |\mathbb{E}[\tilde{Y} \mid X \in L(x)] - \mathbb{E}[\tilde{Y} \mid X = x]| &\leq C \text{diam}^2(L(x)) \\ \mathbb{E}[T(x) - \mathbb{E}[\tilde{Y} \mid X = x]] &= \mathbb{E}[\mathbb{E}[\tilde{Y} \mid X \in L(x)] - \mathbb{E}[\tilde{Y} \mid X = x]] \end{aligned}$$

Let $\eta = 1.25\sqrt{\log((1-\omega)^{-1})} \leq 0.6$. Then $1.98(1-\eta) \geq 0.79$, and $\eta^2/2 \geq 0.78 \log((1-\omega)^{-1})$. Equation 21 gives

$$\mathbb{P}\left(\text{diam}^2(L(x)) \geq \sqrt{d} \left(\frac{s}{2k+1}\right)^{-0.79 \frac{\log((1-\omega)^{-1})}{\log(\omega^{-1})} \frac{\pi}{d}}\right) \leq d \left(\frac{s}{2k+1}\right)^{-0.78 \frac{\log((1-\omega)^{-1})}{\log(\omega^{-1})} \frac{\pi}{d}}$$

The proof of Theorem 3 in [Wager and Athey \[2018\]](#) establishes

$$|\mathbb{E}[T(x)] - \mathbb{E}[\tilde{Y} \mid X = x]| \lesssim d \left(\frac{s}{2k-1}\right)^{-0.78 \frac{\log((1-\omega)^{-1})}{\log(\omega^{-1})} \frac{\pi}{d}} \times \mathcal{O}(1)$$

Since a forest is an average of trees, this bound extends to the bias of the forest. \square

The following two results use the theory of U-statistics to complete the coupling between $\hat{\gamma}_n(x)$ and $\tilde{\gamma}_n(x)$, which relies on appropriately bounding M_λ .

Proof of Lemma 2

Let X_1, \dots, X_n be independent random variables, and recall that a U-statistic takes the form

$$U = \frac{1}{n^{(s)}} \sum_{n,s} g(X_{i_1}, \dots, X_{i_s}),$$

where $\sum_{n,s}$ is over all s -tuples and $n^{(s)} = n!/(n-s)!$. Writing M_λ as

$$M_\lambda = \frac{1}{n^{(s)}} \sum_{n,s} \sum_{i=1}^s \alpha_i \begin{pmatrix} 1 \\ X_i - x \end{pmatrix}^{\otimes 2} + \begin{pmatrix} 0 \\ \lambda \end{pmatrix},$$

we note that every entry of M_λ is a one-dimensional U-statistic. Suppose we have a, b such that $a \leq g(x_1, \dots, x_s) \leq b$. Then, [Hoeffding \[1963\]](#), gives

$$\mathbb{P}(U - \mathbb{E}[U] \geq t) \leq e^{-2 \frac{n}{s} t^2 / (b-a)^2}$$

Let U be any entry of M_λ . Then for any x_1, \dots, x_s , we certainly have $-r_s^2 \leq g(x_1, \dots, x_s) \leq r_s^2$. Hence we may bound $P(U - \mathbb{E}[U] \geq t)$ as

$$P(U - \mathbb{E}[U] \geq t) \leq e^{-\frac{n}{s} t^2 / 2r_s^4}$$

Therefore, across all elements of M_λ ,

$$\begin{aligned} \|M_\lambda - \mathbb{E}[M_\lambda]\|_\infty &= \mathcal{O}_P\left(\sqrt{s/nr_s^2}\right) \\ \|M_\lambda^{-1} - \mathbb{E}[M_\lambda]^{-1}\|_\infty &= \mathcal{O}_P\left(\lambda^{-1}\sqrt{s/nr_s^2}\right) \end{aligned}$$

□

Proof of Corollary 3

From Lemma 2, it follows that

$$\|M_\lambda^{-1} - \mathbb{E}[M_\lambda]^{-1}\|_\infty = \mathcal{O}\left(\lambda^{-1}r_s^2\sqrt{s/n}\right)$$

Clearly $\sum_{i=1}^n \alpha_i(x) \begin{pmatrix} 1 \\ X_i - x \end{pmatrix} \varepsilon_i = \mathcal{O}(1)$, so we have

$$\sum_{i=1}^n \alpha_i(x) M_\lambda^{-1} \begin{pmatrix} 1 \\ X_i - x \end{pmatrix} \varepsilon_i = \sum_{i=1}^n \alpha_i(x) \mathbb{E}[M_\lambda]^{-1} \begin{pmatrix} 1 \\ X_i - x \end{pmatrix} \varepsilon_i + \mathcal{O}\left(\lambda^{-1}r_s^2\sqrt{s/n}\right) \mathcal{O}(1)$$

□

Note that this immediately implies we must choose $\lambda = \mathcal{O}(r_s^2\sqrt{s/n})$.

Proof of Lemma 4

Proving this lemma entails a study of $\tilde{\gamma}_n(x)$. We begin by detailing how honest trees operate under the relevant dependence setup, and then give a central limit theorem at the appropriate subsampling rate.

Recall we have data $(X_1, Y_1), \dots, (X_n, Y_n)$, where $Y_i = \mu(X_i) + \varepsilon_i$, and recall the notation M_λ given in (15). Let

$$S_i = \mathbb{1}\{X_i \in L(x, T)\} / |\{L(x, T)\}|$$

and recall the definition

$$\tilde{Y}_i = e_1^T \mathbb{E}[M_\lambda]^{-1} \begin{pmatrix} 1 \\ X_i - x \end{pmatrix} \varepsilon_i.$$

Then predictions from a tree T are $\sum_{i=1}^n S_i \tilde{Y}_i$. We want to establish that

$$\mathbb{E}[T(x) | X_1] = \mathbb{E}[S_1 | X_1] \mathbb{E}[Y_1 | X_1] \tag{25}$$

In the proof of Theorem 5 from [Wager and Athey \[2018\]](#), honesty automatically provides $\mathbb{E}[S_1 | (X_1, Y_1)] = \mathbb{E}[S_1 | X_1]$, giving (25) immediately. Now, we establish that the relationships shown in [Wager and Athey \[2018\]](#), previously guaranteed by honesty and conditional independence, still hold without independence as long as we have zero correlation. It is sufficient to examine the behavior of one tree T on this problem.

Let us expand the conditional expectation of the tree predictions given X_1 (without loss of generality).

$$\mathbb{E}[T(x) | X_1] = \mathbb{E}\left[\sum_{i=1}^s S_i \tilde{Y}_i | X_1\right] = \mathbb{E}[S_1 \tilde{Y}_1 | X_1] + \sum_{i=2}^s \mathbb{E}[S_i \tilde{Y}_i | X_1]$$

While $\mathbb{E}[M_\lambda]$ and $\alpha_i(x)$ are still not independent, they are crucially uncorrelated given X_1 . Define

$$H_i = S_i e_1^T \mathbb{E}[M_\lambda]^{-1} \begin{pmatrix} 1 \\ X_i - x \end{pmatrix}.$$

Consider first the summation term $\sum_{i=2}^s \mathbb{E}[S_i \tilde{Y}_i | X_1]$. By construction, $\tilde{S}_2 \tilde{Y}_2 = H_2 \varepsilon_2$; and so

$$\begin{aligned} \mathbb{E}[S_2 \tilde{Y}_2 | X_1] &= \mathbb{E}[H_2 \varepsilon_2 | X_1] \\ &= \mathbb{E}[H_2 | X_1] \mathbb{E}[\varepsilon_2 | X_1] \\ &= \mathbb{E}[H_2 | X_1] \mathbb{E}[\varepsilon_2] = 0. \end{aligned}$$

Because S_1, Y_1 are uncorrelated given X_1 , we indeed have $\mathbb{E}[S_1 \tilde{Y}_1 | X_1] = \mathbb{E}[S_1 | X_1] \mathbb{E}[\tilde{Y}_1 | X_1]$. Combining these observations gives Equation (25). Last, we can condition on (X_1, Y_1) and achieve an analogous result through the same steps. Proposition 7 gives a corresponding lower bound on $\text{Var}(T)$. Therefore, Theorem 8 of [Wager and Athey \[2018\]](#) establishes the existence of $\sigma_n(x) \rightarrow 0$ such that

$$\frac{\tilde{\gamma}_n(x) - \mathbb{E}[\tilde{\gamma}_n(x)]}{\sigma_n(x)} \Rightarrow \mathcal{N}(0, 1)$$

We need to show that we can replace $\mathbb{E}[\tilde{\gamma}_n(x)]$ by $\gamma(x) = 0$. Note that any continuity conditions applied to $\mu(x)$ must immediately apply to $\hat{\gamma}_n(x)$. Therefore, Lemma 6 applies. Since $\tilde{\gamma}_n(x)$ is coupled with $\hat{\gamma}_n(x)$, the bias of a tree, and hence of a forest, is

$$|\mathbb{E}[\tilde{\gamma}_n(x)]| = \mathcal{O}\left(n^{-\beta * 0.78 \frac{\log((1-\omega)^{-1})}{\log(\omega^{-1})}}\right)$$

For any $\varepsilon > 0$, [Wager and Athey \[2018\]](#) give the following bound, where k is the minimum leaf size and C is a constant.

$$\sigma_n^2(x) \gtrsim \frac{C}{2k} \frac{s \text{Var}(Y | X = x)}{n \log(s)^d} = \Omega(n^{\beta-1-\varepsilon})$$

Therefore, $\mathbb{E}[\tilde{\gamma}_n(x)]/\sigma_n(x)$ converges to 0 for sufficiently small $\varepsilon > 0$, as long as

$$\beta > 1 - \left(1 + \frac{1}{1.56} \frac{\log(\omega^{-1})}{\log((1-\omega)^{-1})} \frac{d}{\pi}\right)^{-1} = \beta_{\min}$$

□

Proposition 7. *Suppose the conditions of Lemma 4 hold, and moreover that*

$$\left(\mathbb{E}\left[\sum_{i=1}^n H_i\right]\right)^2 \geq \mathcal{O}(1),$$

for H_i as given in the proof of Lemma 4. Moreover, assume that the breakdown $S_i \tilde{Y}_i = H_i \varepsilon_i$ corresponds to $\varepsilon_i = \text{Var}(\tilde{Y}_i | X_i)$. Last, suppose $\text{Var}(\tilde{Y}_i | X_i)$ is equal for all values of i . Then, we have the following bound on $\text{Var}(T)$.

$$\text{Var}(T) \gtrsim \frac{\text{Var}(\tilde{Y} | X = x)}{2k}$$

Proof. We proceed by explicitly computing $\text{Var}(T)$.

$$\text{Var}(T) = \text{Var}\left(\sum_{i=1}^n H_i \varepsilon_i\right) = \sum_{i=1}^n \text{Var}(H_i \varepsilon_i) + 2 \sum_{i=1}^n \sum_{j < i} \text{Cov}(H_i \varepsilon_i, H_j \varepsilon_j)$$

First, observe that $\mathbb{E}[H_i \varepsilon_i] = 0$, thus $\text{Var}(H_i \varepsilon_i) = \mathbb{E}[H_i^2 \varepsilon_i^2]$. One can similarly check that $\mathbb{E}[H_i^2 \varepsilon_i^2] = \mathbb{E}[\mathbb{E}[H_i^2 | X_i] \mathbb{E}[\varepsilon_i^2]] = \mathbb{E}[H_i^2] \text{Var}(\varepsilon_i)$. From the Proposition statement we have assumed that $\text{Var}(\varepsilon_i) = \text{Var}(Y_i | X_i = x) = \text{Var}(Y | X = x)$. Hence,

$$\text{Var}(T) = \sum_{i=1}^n \text{Var}(\tilde{Y} | X = x) \mathbb{E}[H_i^2] + 2 \sum_{i=1}^n \sum_{j < i} \text{Cov}(H_i \varepsilon_i, H_j \varepsilon_j)$$

Quick algebra verifies that $\sum_{i=1}^n \sum_{j < i} \text{Cov}(H_i \varepsilon_i, H_j \varepsilon_j) = 0$. Furthermore, recall that $H_i = 0$ if $S_i = 0$, so $\sum_{i=1}^n H_i$ is a sum of $|\{i : X_i \in L(x)\}|$ nonzero terms. The Cauchy-Schwartz inequality then gives

$$\sum_{i=1}^n \mathbb{E}[H_i^2] \geq \frac{1}{|\{i : X_i \in L(x)\}|} \left(\sum_{i=1}^n \mathbb{E}[H_i] \right)^2$$

Recall that $\text{Var}(T) = \text{Var}(\sum_{i=1}^n H_i \varepsilon_i)$. Expanding to $\text{Var}(\tilde{Y} | X = x) \sum_{i=1}^n \mathbb{E}[H_i^2]$, and noting the assumed bound on $(\mathbb{E}[\sum_{i=1}^n H_i])^2$,

$$\begin{aligned} \text{Var}(T) &\geq \frac{\text{Var}(\tilde{Y} | X = x)}{|\{i : X_i \in L(x)\}|} \left(\mathbb{E} \left[\sum_{i=1}^n H_i \right] \right)^2 \\ &\gtrsim \frac{\text{Var}(\tilde{Y} | X = x)}{2k}. \end{aligned}$$

This establishes the necessary lower bound on $\text{Var}(T)$. \square

Proof of Lemma 5

Recall from (18) that we can decompose $\hat{\mu}_n(x)$ with dominating bias term

$$\delta_1(x) = \sum_{i=1}^n e_1^T M_\lambda^{-1} \begin{pmatrix} 1 \\ X_i - x \end{pmatrix} \alpha_i \nabla \mu(x) \begin{pmatrix} 0 \\ X_i - x \end{pmatrix}^T$$

Define the weighted average and corresponding centered matrix

$$\begin{aligned} \bar{X} &:= \sum_{i=1}^n \alpha_i(x) X_i \\ X_c &:= X - \bar{X} \end{aligned}$$

Then write $\delta_1(x)$ as a function of a vector ν , where

$$\delta_1(\nu) = X_C (I - (X_C^T A X_C + \lambda I)^{-1} X_C^T A X_C) \nu,$$

for $\nu = (0 \quad \nabla \mu(x))^T$. Last, define

$$B = I - (X_C^T A X_C + \lambda I)^{-1} X_C^T A X_C, \quad (26)$$

so that $\delta_1(\nu) = X_C B \nu$. We must bound $\delta_1(\nu)$ in probability, and hence can restrict to $\|\nu\|_2 \leq 1$. Moreover, we know $\|X_C\|_2 \leq \mathcal{O}(r_s)$, where r_s is given in equation 21. Recall the definition of the matrix operator norm

$$\|B\|_{op} = \inf\{c \geq 0 : \|B\nu\|_2 \leq c\|\nu\|_2 \text{ for all } \nu \in \mathbb{R}^{p+1}\} = \|B\|_*, \quad (27)$$

where $\|B\|_*$ is the largest eigenvalue of $B^T B$. By this definition, we can clearly bound

$$\sup_{\nu: \|\nu\|_2 \leq 1} \|\delta_1(\nu)\|_2 \leq \|B\|_* \mathcal{O}(r_s). \quad (28)$$

Let $M = X_C^T A X_C$ and write the operator matrix B from (26) as

$$B = I - (M + \lambda I)^{-1} M \quad (29)$$

First, suppose $\lambda = 0$. Then $B = I - M^{-1} M = I$, and corresponding first-order error is $\delta_1(\nu) = X_C(I - I)\nu = 0$. Therefore any probability bound for nonzero λ will trivially hold for this case. More importantly, note this intuition; if $\lambda = 0$, we do not apply a ridge correction, and hence do not incur the subsequent first-order bias.

Let σ_i be the eigenvalues of M . For nonzero λ , basic linear algebra verifies that the eigenvalues of $(M + \lambda I)^{-1} M$ are $\frac{\sigma_i}{\sigma_i + \lambda}$, and hence that the eigenvalues of B are

$$\frac{\lambda}{\lambda + \sigma_i} \quad (30)$$

Therefore,

$$\|B\|_* = \max_{\sigma_i} \left\{ \frac{\lambda}{\lambda + \sigma_i} \right\}$$

Certainly $\frac{\lambda}{\lambda + \sigma_i}$ is maximized at the smallest value of σ_i , which corresponds to the smallest eigenvalue of $M = X_C^T A X_C$, and the inverse of the largest eigenvalue of M^{-1} . That is,

$$\|B\|_* = \frac{\lambda}{\lambda + (\|M^{-1}\|_*)^{-1}}$$

Recall that we assumed $\lambda = \mathcal{O}(r_s^2 \sqrt{s/n})$. As $\|M^{-1}\|_* = \|(X_C^T A X_C)^{-1}\|_* = \mathcal{O}(1/r^2)$, we have $\|B\|_* = \mathcal{O}(\lambda r_s / (\lambda + r_s^2)) = \mathcal{O}(\lambda / r_s)$. By our choice of λ , we have $\mathcal{O}(\lambda / r_s) = \mathcal{O}(r_s \sqrt{s/n})$. Equation 21 then yields the final bound

$$\delta_1 = \mathcal{O}(r_s \sqrt{s/n}) = \mathcal{O} \left(n^{-\beta \frac{0.78}{2} \frac{\log((1-\omega)^{-1})}{\log(\omega^{-1})} \frac{\pi}{4} n^{(\beta-1)/2}} \right).$$

□